Flow interaction with dynamic vegetation patches: Implications for biogeomorphic evolution of a tidal landscape

W. Vandenbruwaene,[1] S. Temmerman,[1] T. J. Bouma,[2] P. C. Klaassen,[2] M. B. de Vries,[3] D. P. Callaghan,[2,4] P. van Steeg,[3] F. Dekker,[3] L. A. van Duren,[3] E. Martini,[3] T. Balke,[2] G. Biermans,[1] J. Schoelynck,[1] and P. Meire[1]

Received 1 June 2010; revised 1 November 2010; accepted 29 November 2010; published 16 February 2011.

[1] Feedback between vegetation growth, water flow, and landform is important for the biogeomorphic evolution of many landscapes, such as tidal marshes, alluvial rivers, and hillslopes. While experimental studies often focus on flow reduction within static homogeneous vegetation, we concentrate on flow acceleration around and between dynamically growing vegetation patches that colonize an initially bare landscape, with specific application to *Spartina anglica*, a pioneer of intertidal flats. *Spartina* patches were placed in a large-scale flow facility of 16 × 26 m, simulating the growth of two vegetation patches by increasing the patch diameter (D = 1–3 m) and decreasing the interpatch distance (d = 2.3–0 m). We quantified that the amount of flow acceleration next to vegetation patches, and the distance from the patch where maximum flow acceleration occurs, increases with increasing patch size. In between the patches, the accelerated flow pattern started to interact as soon as $D/d \geq 0.43$–0.67. As the patches grew further, the flow acceleration increased until $D/d \geq 6.67$–10, from which the flow acceleration between the patches was suppressed, and the two patches started to act as one. These findings are in accordance with theory on flow around and between nonpermeable structures; however, the threshold D/d values found here for permeable vegetation patches are higher than those for nonpermeable structures. The reported flow interactions with dynamic vegetation patches will be essential to further understanding of the larger-scale biogeomorphic evolution of landscapes formed by flowing water, such as tidal flats, floodplain rivers, and hillslopes.

Citation: Vandenbruwaene, W., et al. (2011), Flow interaction with dynamic vegetation patches: Implications for biogeomorphic evolution of a tidal landscape, *J. Geophys. Res.*, *116*, F01008, doi:10.1029/2010JF001788.

1. Introduction

[2] Recent studies emphasize that two-way interactions between biological and physical processes, so-called *biogeomorphic* feedback, play a key role in the formation and evolution of many landscapes (see *Corenblit et al.* [2008] and *Murray et al.* [2008] for a recent review). For example, the establishment of vegetation in an initially bare landscape modifies the patterns of water and airflow and of sedimentation and erosion, while the modified flow and sedimentation-erosion patterns influence the spatial patterns of vegetation establishment and dieback. These kinds of biological-physical feedback seem to determine the formation of both vegetation and landform patterns as landscapes evolve from a bare state to a vegetated state, or vice versa. This has been recently demonstrated for a number of landscape types, such as intertidal landscapes [e.g., *D'Alpaos et al.*, 2007; *Kirwan and Murray*, 2007; *Marani et al.*, 2007; *Temmerman et al.*, 2007], alluvial river channels and floodplains [e.g., *Murray and Paola*, 2003; *Tal and Paola*, 2007], dune landscapes [e.g., *Baas and Nield*, 2007], and hillslopes [e.g., *Collins et al.*, 2004; *Istanbulluoglu and Bras*, 2005].

[3] Most of the studies mentioned above are based on simulation modeling, while limited empirical data exist on the plant-flow feedback that occurs when an initially bare landscape is colonized by patchy vegetation that dynamically grows in time. Flow hydrodynamics have been traditionally studied within homogeneous, static vegetation in flumes [e.g., *Nepf and Vivoni*, 2000; *Shi et al.*, 1995, 1996] and in the field [e.g., *Leonard and Luther*, 1995; *Leonard and Croft*, 2006; *Neumeier and Amos*, 2006]. Such studies support the classical view that vegetation reduces flow velocities and hence reduces erosion and promotes sedimentation. However, in the case of patchy vegetation, recent flume and field studies have shown that more

[1]Department of Biology, University of Antwerp, Antwerp, Belgium.
[2]Centre for Estuarine and Marine Ecology, Netherlands Institute of Ecology, Yerseke, Netherlands.
[3]Deltares, Delft, Netherlands.
[4]Now at School of Civil Engineering, University of Queensland, Brisbane, Queensland, Australia.

0148-0227/11/2010JF001788

complex, so-called scale-dependent feedback occurs [*Bouma et al.*, 2009; *Temmerman et al.*, 2007; *van Wesenbeeck et al.*, 2008]: at a small scale, *within* the vegetation patches, flow velocities and erosion are indeed reduced, and it has been experimentally demonstrated that this results in improved plant growth (positive feedback) [*van Wesenbeeck et al.*, 2008]; but at a larger scale, the water is partly forced to flow *around* the vegetation patches, leading there to increased flow velocities, to erosion [*Bouma et al.*, 2007], and to inhibition of plant growth just next to the vegetation patch (negative feedback) [*van Wesenbeeck et al.*, 2008] (Figure 1a). Although scale-dependent feedback around static vegetation patches has been empirically demonstrated [*Bouma et al.*, 2009; *van Wesenbeeck et al.*, 2008], it is not known yet how dynamic vegetation patches, which grow in size and consequently come closer to each other, affect the *strength* of the scale-dependent feedback. In other words, the effect of patch size and interpatch distance on the flow acceleration around vegetation patches is not yet understood.

[4] It has been shown that scale-dependent feedback between organisms and their environment results in the self-organization of regular spatial patterns in a broad range of ecosystems (see *Rietkerk and Van de Koppel* [2008] for an overview). Recently, there have been strong indications that scale-dependent feedback is also crucial for the formation of landscapes that are affected by flowing water and that are colonized by patchy dynamic vegetation. For example, aerial photographs and modeling of an intertidal landscape suggest that colonization of a bare mudflat by laterally expanding vegetation patches results in sediment accretion within the vegetation patches and at the same time channel erosion in between the growing vegetation patches (Figure 1b, ellipse). The model suggests that, through this mechanism, an initially bare mudflat with few or no channels evolves into a vegetated marsh platform dissected by a regular pattern of channels [*Temmerman et al.*, 2007]. Similarly, a scaled flume study demonstrated that an unvegetated river floodplain with a braiding pattern of multiple shallow channels may develop by plant colonization into a vegetated floodplain with a single deep river channel [*Tal and Paola*, 2007]. Here we stress that flow reduction within vegetation patches together with flow acceleration in between laterally growing vegetation patches is the key mechanism that is responsible for the shift between unvegetated and vegetated landscape states. Therefore, it is crucial to quantify the amount of flow acceleration around and between growing vegetation patches,

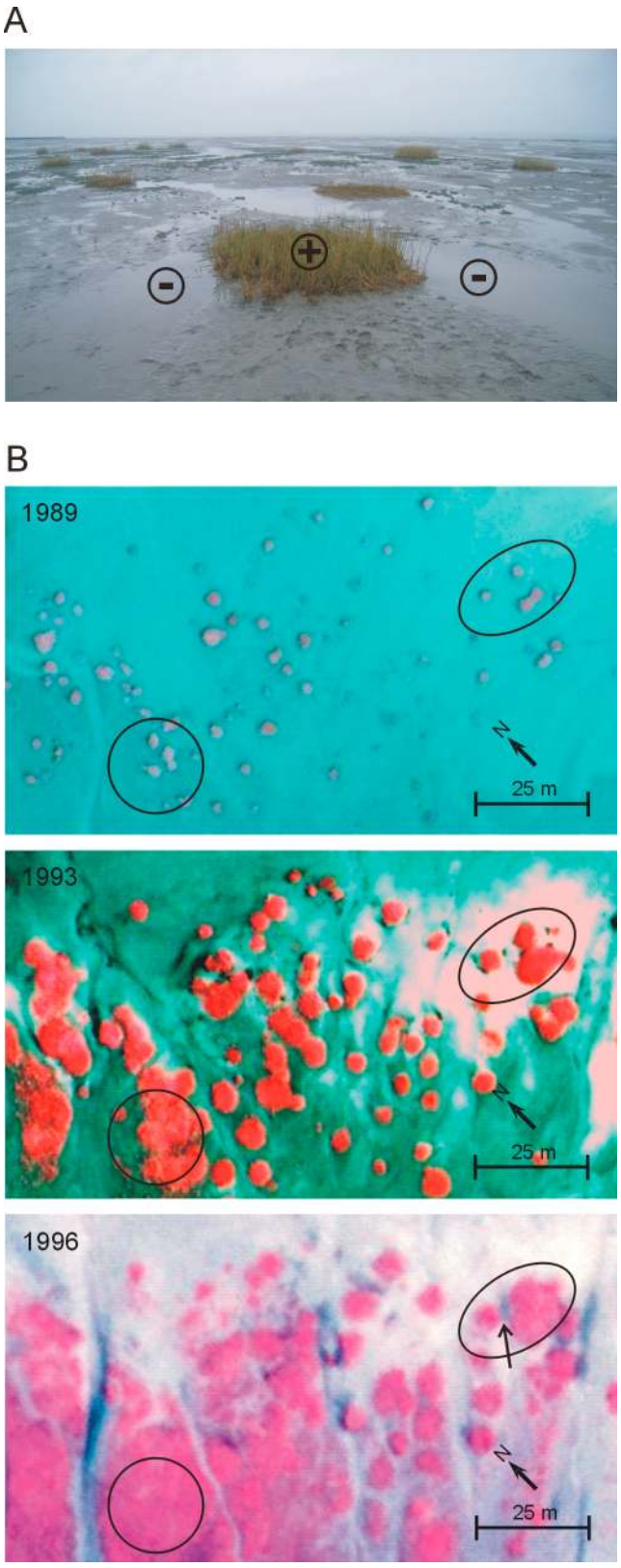

Figure 1. (a) Scale-dependent feedback around a vegetation patch in an intertidal landscape (*S. anglica* patches, SW Netherlands). The positive feedback within the vegetation patch leads to flow reduction, sediment accretion, and improved plant growth. The negative feedback around the patch results in flow acceleration and erosion, which negatively affects the plant growth conditions. (b) Aerial photographs showing the evolution of an intertidal landscape in time (SW Netherlands). The lateral expansion of patches results in an increase of patch size and a decrease of interpatch distance (compare 1989 and 1993, patches within ellipse). In between the growing patches, erosion may occur, resulting in channel initiation and a stop in the lateral patch expansion (compare 1993 and 1996, patches within ellipse, arrow points toward a pool, initiated by erosion in between the patches). The circle shows the growth of neighboring patches that merge into a closed vegetation field.

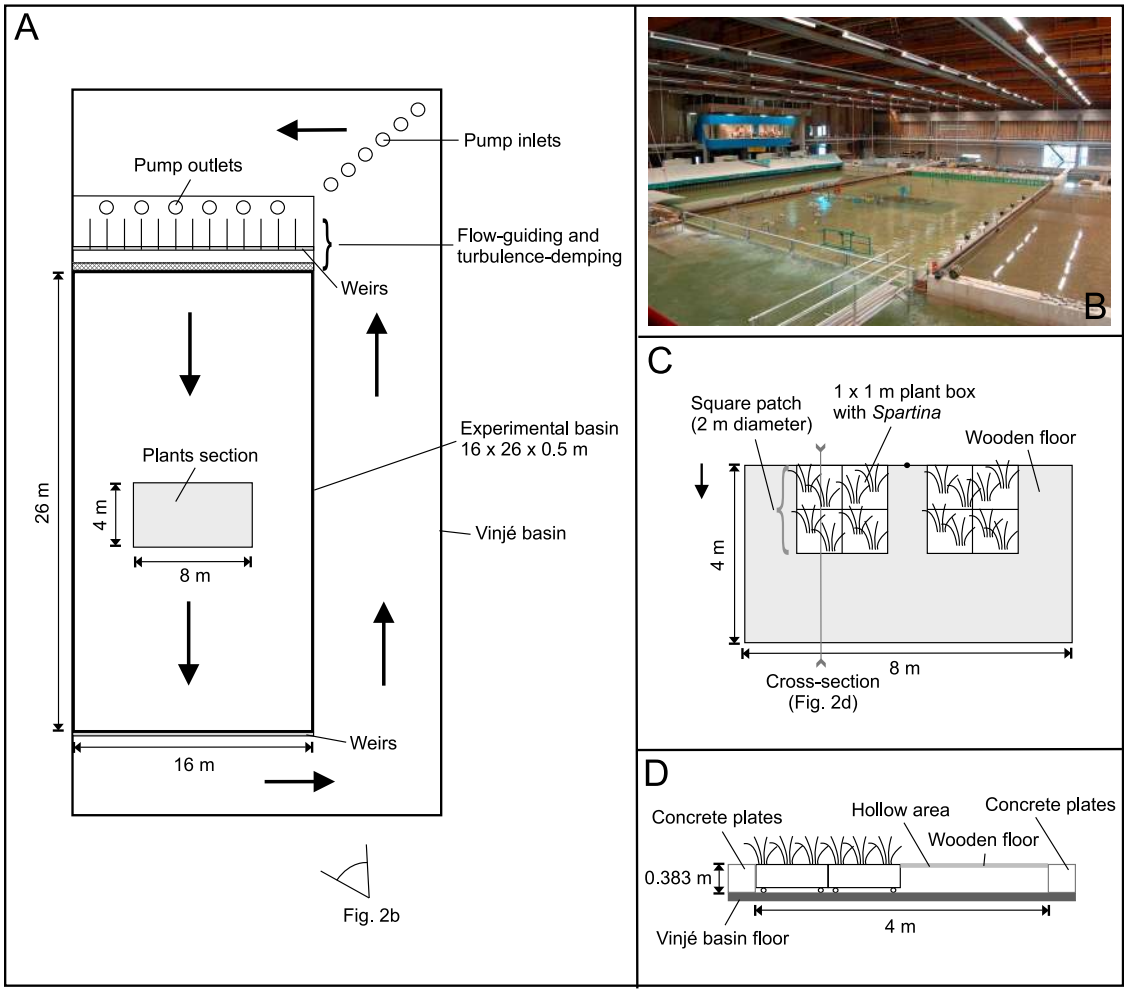

Figure 2. (a) Top view of the design of the flow facility. (b) Overview picture of the flow facility. (c) Top view of the central area of the flow facility, used for construction of different patch configurations. (d) Cross section of the central area (see Figure 2c), showing in which way patch configurations were created.

as a function of patch size and interdistance. After all, the amount of flow acceleration will determine whether channels start to erode around the patches, and whether further lateral patch growth will be inhibited.

[5] Scouring by flow acceleration around nonpermeable flow-blocking structures, such as piles, piers, and abutments, has been extensively studied for a wide range of pile group arrangements [e.g., *Ataie-Ashtiani and Beheshti*, 2006; *Melville*, 1997; *Melville and Chiew*, 1999; *Oliveto and Hager*, 2002]. When piles are placed close to each other, the surrounding accelerated flow patterns start to interact in between adjacent piles. It has been demonstrated that this interaction initiates when the ratio between pile diameter (D) and pile interdistance (d) becomes larger than a critical value ($D/d > 0.25$–0.5) [*Ataie-Ashtiani and Beheshti*, 2006]. This study further showed that piles act as a single pile (i.e., flow acceleration in between the piles is suppressed) as soon as a second, larger critical value of D/d is exceeded ($D/d > 4$).

[6] In accordance with this general theory on flow around nonpermeable structures (piles), we hypothesize that flow acceleration around vegetation patches increases with increasing patch size. Furthermore, we expect that the accelerated flow starts to interact between two adjacent, laterally expanding vegetation patches, as soon as a first critical value of D/d is exceeded. As the vegetation patches further grow, and D/d further increases, we hypothesize that the two vegetation patches start to act as one, as a second, larger critical D/d value is exceeded. Although this theory has been supported by experimental data for nonpermeable structures [*Ataie-Ashtiani and Beheshti*, 2006], there are no experimental data yet on vegetation patches. We presume that the critical D/d values for vegetation patches will be larger than for nonpermeable structures, due to the permeability of the vegetation patches.

[7] In this study we focus on vegetation patches that colonize an intertidal landscape. *Spartina* species are very common colonizers (*S. anglica* in northwestern Europe; *S. alterniflora* in North America and Asia). After initial establishment of *Spartina* seedlings, the plants form circular patches due to lateral clonal growth [*Callaway and Josselyn*, 1992; *Hubbard*, 1965; *Sanchez et al.*, 2001]. This means that during the colonization process the size of patches increases and at the same time the interpatch distance

Table 1. Overview Table of the Experimental Setup[a]

Experimental Configuration	Number of Patches	Patch Diameter (m)	Interpatch Distance (m)	Incoming Flow Velocity (m/s)	Experimental Series
1 m_{patch}-2.3 $m_{distance}$	2	1	2.3	0.3	1
2 m_{patch}-1.3 $m_{distance}$	2	2	1.3	0.3	1, 3
3 m_{patch}-0.3 $m_{distance}$	2	3	0.3	0.3	1, 2
1 m_{patch}-0.3 $m_{distance}$	2	1	0.3	0.3	2
2 m_{patch}-0.3 $m_{distance}$	2	2	0.3	0.3	2, 3
2 m_{patch}-3 $m_{distance}$	2	2	3	0.1, 0.2, 0.3	3, flow
2 m_{patch}-0 $m_{distance}$	2	2	0	0.3	3
2 m_{patch}-square	1	2	–	0.3	shape
2 m_{patch}-circular	1	2	–	0.3	shape

[a]Each patch configuration is part of one or two experimental series. In total, there were three experimental series: (1) effect of increasing patch diameter and decreasing interpatch distance, (2) effect of varying patch size and constant interdistance, and (3) effect of constant patch size and varying interdistance. Two additional experiments were carried out to test the effect of patch shape (shape) and different incoming flow velocity (flow). The numbers in the notation of the experimental configurations refer to the corresponding patch diameter and the corresponding interpatch distance.

decreases. Aerial photographs indicate that, at some locations between expanding vegetation patches, channels may start to erode and further lateral growth of the vegetation patches may stop (Figure 1b, ellipse), while at other locations patches may merge together and form bigger *Spartina* fields (Figure 1b, circle) [*Temmerman et al.*, 2007]. The latter suggests that the flow acceleration around expanding vegetation patches may be suppressed if the patches get close enough to each other, something that has not been tested yet.

[8] Here we present the results of a large-scale flume study, in which field-scale *Spartina anglica* patches (1–3 m diameter) were placed in a large-scale flow facility (16 × 26 m). The aim of this study was to quantify the effects of increasing patch size and decreasing interpatch distance on the amount of flow acceleration next to and in between the patches. The experimental results are interpreted in terms of implications for the biogeomorphic evolution of an intertidal landscape that is colonized by patchy *Spartina* vegetation.

2. Methods

2.1. The Flow Facility

[9] The experimental facility was developed at Deltares (www.deltares.nl, Delft, Netherlands), within the so-called Vinjé basin. The facility consisted of an experimental basin 16 m wide, 26 m long, and 0.5 m deep, in which a uniform, unidirectional flow was generated (Figures 2a and 2b). Six pumps, with a total maximum discharge of 1.44 $m^3\ s^{-1}$, were used for circulation of the water. In order to break down the turbulence generated by the pumps and to achieve a steady, homogeneous flow in the experimental basin, several flow-guiding and turbulence-damping structures were placed in between the pumps and the upstream edge of the experimental basin (Figure 2a). The water depth and flow velocity in the experimental basin were controlled by changing the height of the 16 weirs at the upstream edge and the five weirs at the downstream edge of the basin and by changing the discharge of the pumps. For all experiments, water depth and flow velocity in the experimental basin were kept at 0.3 m and 0.3 m/s, respectively, a representative flow velocity value for maximal tidal currents as observed on the intertidal flats in the Westerschelde estuary (Netherlands) [*Bouma et al.*, 2005; *Temmerman et al.*, 2005]. To cover the whole range of intertidal flow velocities, additional experiments were done at 0.1 and 0.2 m/s. The floor of the experimental basin consisted of flat concrete, with the exception of a central hollow area of 8 × 4 m that was used for placement of plant boxes or that could be covered by wooden plates (see Figures 2c and 2d).

2.2. Plants

[10] *Spartina anglica* plants were grown in boxes with a surface area of 1 × 1 m and a depth of 0.2 m. The boxes were first filled to the top with sediment consisting of silty sand. In open air and with irrigation of salt water, the *S. anglica* plants were subsequently grown from seeds. Just before the start of each experiment, the plant boxes were moved to the flow basin and sunk into the floor of basin, by partial removal of the wooden floor in the center of the basin. In this way the top of the sediment surface in the plant boxes was always at the same level as the surrounding floor of the basin (Figures 2c and 2d). By moving and combining more or fewer plant boxes, *Spartina* patches with different sizes and different interdistances were formed.

[11] After the experiments the *Spartina anglica* vegetation of four plant boxes was harvested to determine plant characteristics. The vegetation was emergent and had a mean stem height of 0.59 ± 0.18 m, a shoot density of 658 ± 8 stems/m^2, and a standing biomass of 580 ± 49 g/m^2. These values are representative of field conditions [*Van Hulzen et al.*, 2007]. The mean shoot diameter at the base was 0.043 ± 0.012 m, and halfway up was 0.03 ± 0.011 m.

2.3. Different Patch Configurations

[12] In all experiments, two *Spartina* patches were placed next to each other along a cross section perpendicular to the incoming flow direction (see Figure 2c). Three series of experiments were carried out (see Table 1 for an overview). The first series mimics the lateral growth of *Spartina* patches as it occurs in the field when patches colonize a tidal flat, by a combination of increasing patch diameter and at the same time decreasing interpatch distance (Figures 3a–3c). In order to separate the effect of patch size and interdistance, a second series of experiments was performed with a constant interpatch distance and varying patch size (Figures 3c–3e), and a third series with constant patch size and varying interpatch distance (Figures 3b, 3e, 3f, and 3g).

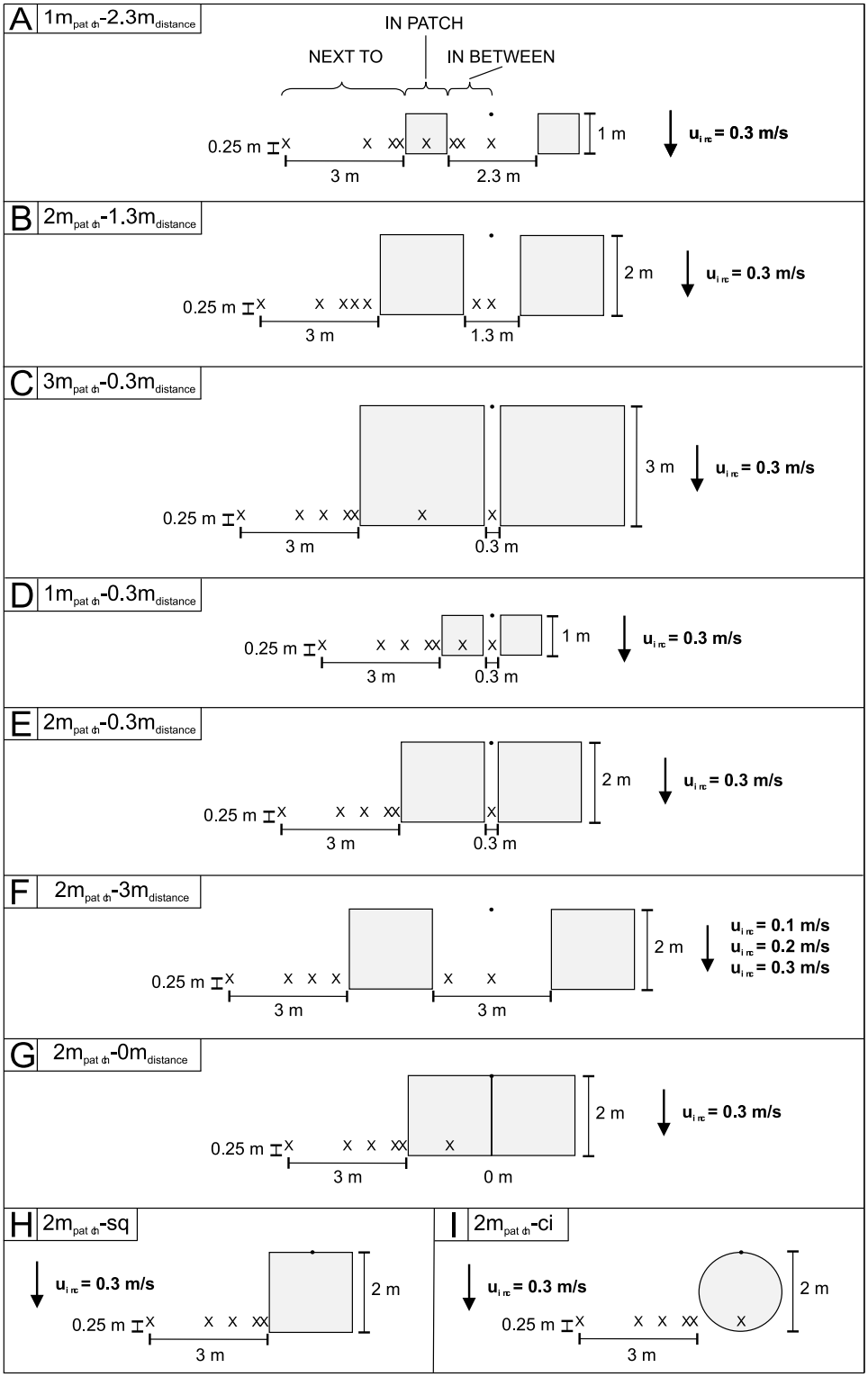

Figure 3. Overview of all patch configurations used in the experiments with indication of patch size and interpatch distance, flowmeter positions (crosses), and incoming flow velocity.

2.4. Patch Shape and Incoming Flow Velocity

[13] The patches in our experiments were square to allow the quick building and breaking down of different patch configurations. However, in the field, individual patches have circular shapes. To determine the effect of patch shape on our results, we compared a square patch versus a circular patch (Figures 3h and 3i and Table 1).

[14] During the experiments, the incoming flow velocity was always 0.3 m/s, except for one patch configuration

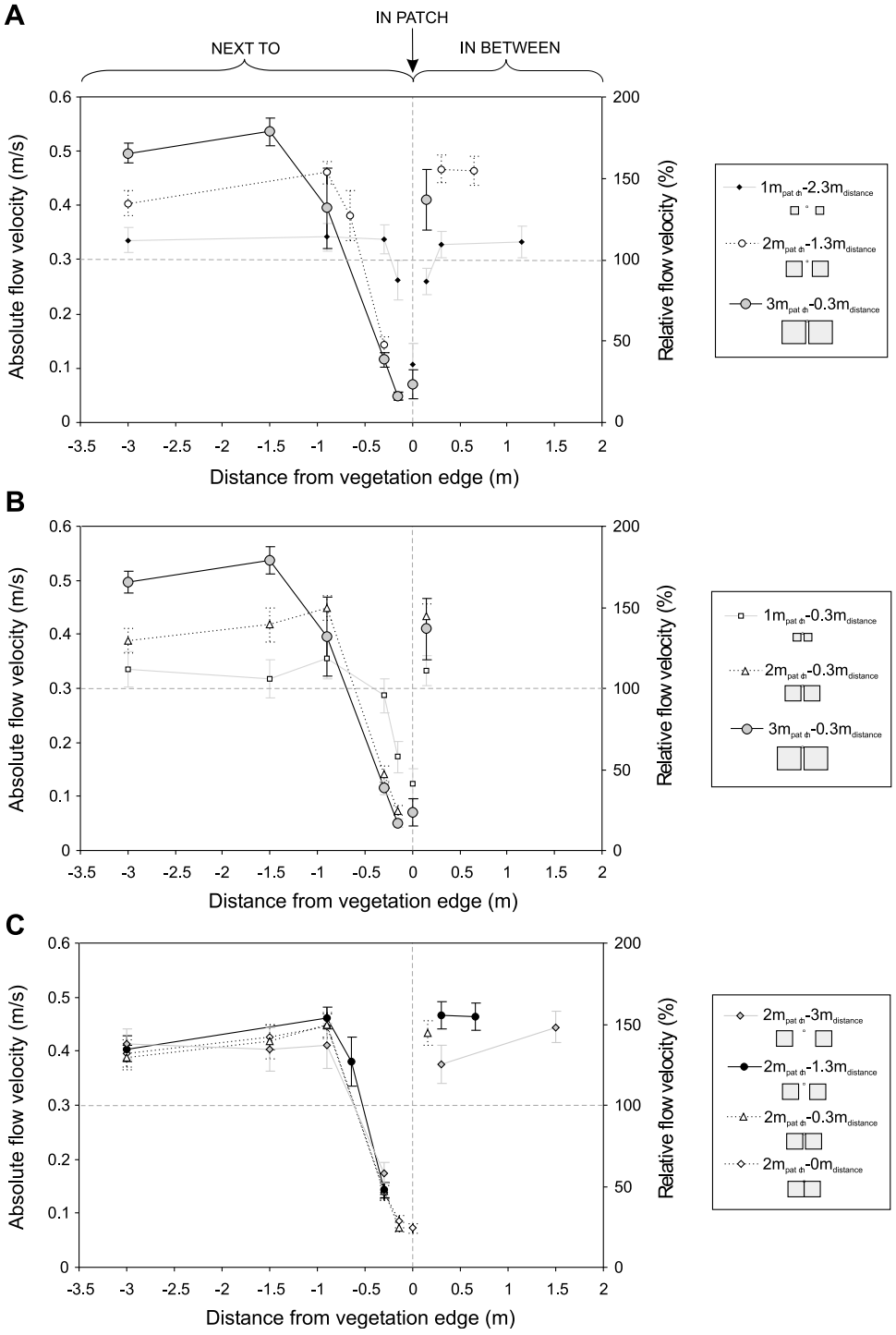

Figure 4. Time-averaged flow velocities with standard deviations (error bars), measured on locations (symbols) next to, in between, and in the patches for the three experimental series. Flow velocities (in m/s on left *Y* axis; in percent of incoming flow velocity on right *Y* axis) are plotted against the distance from the vegetation edges (m), with the 0 value representing the entire patch width. The incoming flow velocity was 0.3 m/s and is represented by the horizontal dashed line. Flow velocities in the patches are plotted on the vertical dashed line. (a) Combination of increasing patch size and decreasing interdistance. (b) Increasing patch size and constant interdistance. (c) Decreasing interpatch distance and constant patch size.

where additional runs were done at 0.1 and 0.2 m/s (Figure 3f and Table 1).

2.5. Measuring Flow Velocities

[15] For all experimental runs, flow velocities and directions were measured with 10 electromagnetic flowmeters (EMFs) (manufactured by Deltares, frequency 25 Hz) and one acoustic Doppler velocimeter (ADV) (Nortek Vector, frequency 25 Hz). Two flowmeters measured the incoming flow velocity at 5 m in front of the patches, while the other flowmeters were placed along a cross section next to the patch, in the patch, and in between the patches (Figure 3a). As the patch configurations were changed, the positions of the flowmeters relative to the vegetation edges were kept constant (Figure 3). At all locations, flow velocity was measured 0.12 m above the bottom surface. Test runs, in which vertical flow velocity profiles were measured, revealed that the flow velocity measurement at 0.12 m above the bottom is representative of the depth-averaged flow velocity. All flow velocities presented in the results section are time-averaged data over a period of about 12 min, with the error bars indicating the standard deviations about the mean.

2.6. Dimensionless Analyses

[16] To combine the data from different patch configurations, and in this way interpret our results in a more general way, several dimensionless parameters were introduced. First, the effect of patch diameter (D) on the maximum flow velocity (u_{max}) next to a vegetation patch was studied by plotting the D/h ratio (h = the water depth) against the dimensionless maximum flow velocity u_{max}/u_{inc} (u_{inc} = the incoming flow velocity). Second, the distance from the vegetation edge d_{ve} was written in a dimensionless form (1) by dividing d_{ve} by the patch diameter (d_{ve}/D) for measuring locations next to vegetation patches and (2) by dividing d_{ve} by the interpatch distance (d_{ve}/d) for measuring locations in between vegetation patches. The spatial variations in measured flow velocities (u) were analyzed then by plotting d_{ve}/D and d_{ve}/d against the dimensionless measured flow velocity u/u_{max}. Finally, we wanted to assess the effect of patch growth on the degree of flow interaction in between the patches. Therefore, as a measure for patch growth the ratio of patch diameter and interpatch distance (D/d) was plotted against a measure for flow interaction, defined here as the difference in flow velocity next to the patches (u_n) and in between the patches (u_b), both measured at the same distance from the vegetation edge, written in dimensionless form as $(u_b - u_n)/u_{inc}$. We thus speak of flow interaction in between patches when the spatial flow patterns next to and in between the patches become asymmetrical.

3. Results

3.1. Combination of Increasing Patch Size and Decreasing Interdistance

[17] For the smallest patch size (1 m diameter) with largest interpatch distance (2.3 m), there is a strong reduction of flow velocity (up to 35% of the incoming flow velocity) within the vegetation patch (Figure 4a). Next to and in between the patches, there is also a small decrease in flow velocity close to the vegetation edges (at 0.15 m), but an increase of up to 113% further from the edges. The increase remains constant over the rest of the cross section. The flow patterns next to and in between the patches are the same, demonstrating that the two patches are still far from each other and do not have an interactive effect yet on the flow between the patches.

[18] After the patch size has grown to 2 m, and the interpatch distance decreased accordingly to 1.3 m, the flow is increasingly accelerated next to and between the patches (up to 154%) (Figure 4a). This increase in flow velocity is larger than for the previous configuration with smaller patches. Next to the patches, close to the vegetation edge, there is first a reduction in flow velocity (less than 50% at 0.3 m), while only farther from the vegetation edge the flow velocity increases to a maximum value of 152% at 0.9 m. In between the patches, however, there is no reduction in flow velocity at 0.3 m from the vegetation edge. Instead, the flow velocity is directly increased to a maximum value of 154%, which is comparable with the maximum value next to the patch. Hence, the flow patterns next to and in between the patches are no longer symmetrical, demonstrating that the two patches have come so close now that an interactive effect occurs resulting in strong flow concentration in between the patches.

[19] For the configuration with the largest patch size (3 m) and smallest interpatch distance (0.3 m), the maximum flow velocity next to the patches was increased even more up to 181% (Figure 4a). Next to the patches, close to the vegetation edge (at 0.15 and 0.3 m), flow velocities are reduced, while farther from the edge (at 1.5 and 3 m) the flow velocity is increased toward the largest values (respectively 167% and 181%). The increase in flow velocity in between the patches (up to 138%) is much lower now than the maximum flow velocity next to the patch (181%). This is even better illustrated when plotting the maximum flow velocities next to and in between the patches as a function of the patch growth (Figure 5a). Next to the patches the maximum flow velocity increases with increasing patch size and decreasing interdistance. In between the patches the same relationship is found when the patches grow from 1 to 2 m in diameter, but when the patches grow bigger and closer to each other, the flow velocity between the patches again decreases. The latter demonstrates that the two patches interact now in such a way that they start to act as one obstacle that the water is forced to flow around.

3.2. Increasing Patch Size, Constant Interdistance

[20] To distinguish the effect of patch size from the effect of interpatch distance, a second series of experiments was carried out in which we varied patch size while maintaining a constant interdistance (Figure 4b). To avoid potentially artificial flow concentration caused by a nearby flow facility wall (especially the case for the largest patch size), a small interdistance of 0.3 m was chosen. Similar to the previous experiment, we observe a reduction in flow velocity next to the patches, close to the vegetation edge, and an increase in flow velocity farther from the edge (Figure 4b). As in the previous experiment, the maximum flow velocity next to the patches increases with the patch size (Figure 5b, compare Figures 5b and 5a). In between the patches, there is never flow reduction close to the vegetation edge, only flow acceleration (Figure 4b). Hence the flow patterns next to and

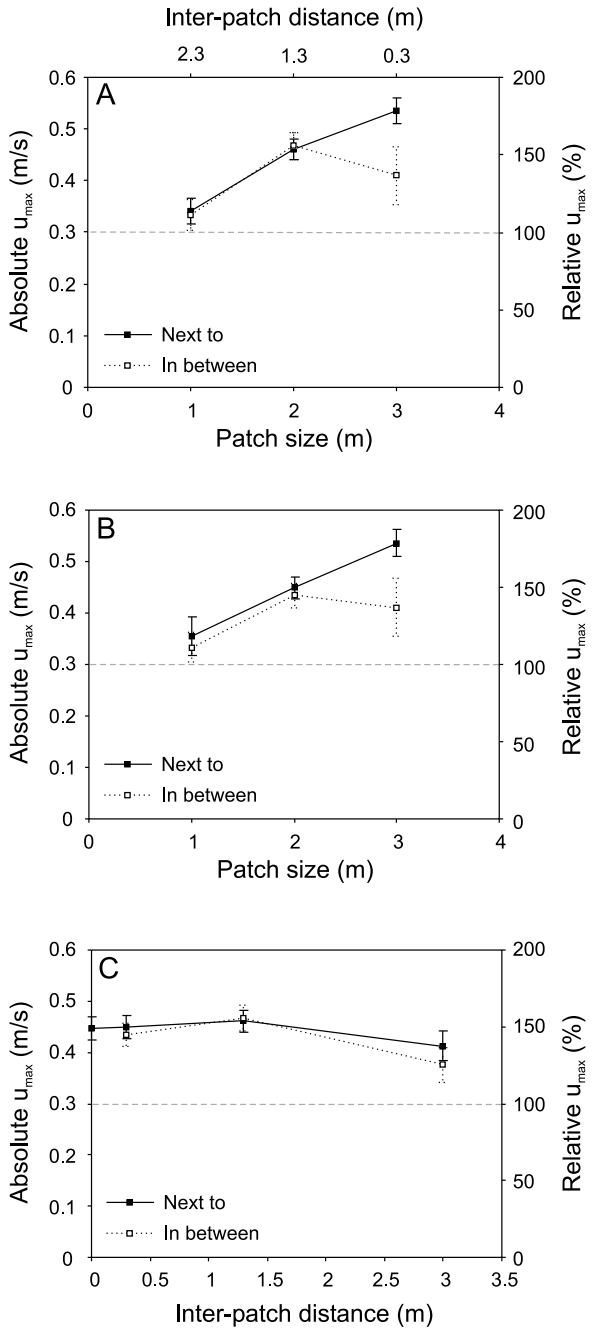

Figure 5. Comparison of maximum flow velocity (m/s and %) next to and in between the patches for the three experimental series. (a) Effect of increasing patch size and decreasing interdistance. (b) Effect of increasing patch size and constant interdistance. (c) Effect of decreasing interpatch distance and constant patch size.

in between the patches are asymmetrical, because the patches are always close to each other (0.3 m interdistance). The maximum flow velocity next to and in between the patches is similar for the 1 and 2 m patch sizes (Figure 5b), but for the 3 m patch size the velocity is smaller in between than next to the patches, demonstrating that the two patches start to act as one object as they become bigger than 3 m in size.

3.3. Decreasing Interpatch Distance, Constant Patch Size

[21] To assess the effect of interpatch distance, a third series of experiments was performed with a constant patch size of 2 m and varying interdistance. Regardless of the interpatch distance, the flow patterns next to the patches are not significantly different (Figure 4c). As observed for the previous experiments, there is always a reduction of flow velocity close to the vegetation edge, while further from the edge, the flow velocity increased, in this series toward a maximum of about 154% at 0.9 m. In between the patches the flow is accelerated to a maximum of 156% and there is no flow reduction close to the vegetation edges as it occurs next to the patches. The maximum flow velocities vary little with changing interpatch distance and are comparable in between and next to the patches (Figure 5c).

3.4. Effect of Patch Size on the Maximum Flow Velocity

[22] We observed that the maximum flow velocity next to the patches is related to the patch size (Figures 5a and 5b). By plotting all maximum flow velocities, written in a dimensionless form as $u_{\max,n}/u_{inc}$, against the dimensionless patch diameter D/h (Figure 6), the following relationship was found:

$$\frac{u_{\max,n}}{u_{inc}} = \exp\left(a\frac{D}{h}\right), \tag{1}$$

where $u_{\max,n}$ is the maximum flow velocity next to the patch (m/s), u_{inc} is the incoming flow velocity (m/s), D is the patch diameter (m); h is the water depth (m), and a is a regression coefficient. In this case, next to a square *Spartina anglica* patch, $a = 0.058$ ($R^2 = 0.94$; $p < 0.0001$) (Figure 6, solid line). In between the patches this relationship is valid for $D/h = 3.33$ and $D/h = 6.67$; however, for $D/h = 10$ the corresponding $u_{\max,n}/u_{inc}$ value clearly plots below the trend line (Figure 6).

3.5. Quantifying Scale-Dependent Feedback

[23] Our observations showed that next to vegetation patches a typical flow patterning occurs: close to the vegetation

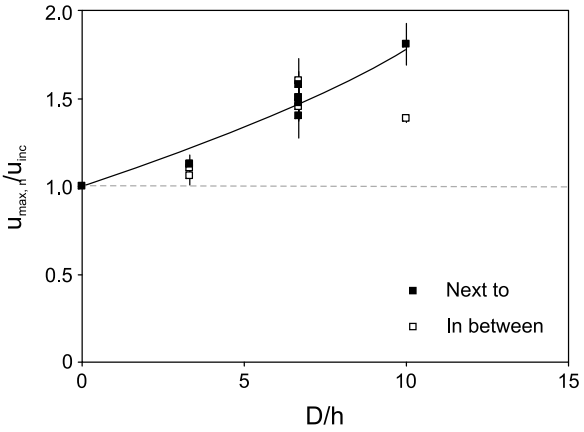

Figure 6. Dimensionless representation of the effect of patch size on the maximum flow velocity, including the case $D/h = 0$.

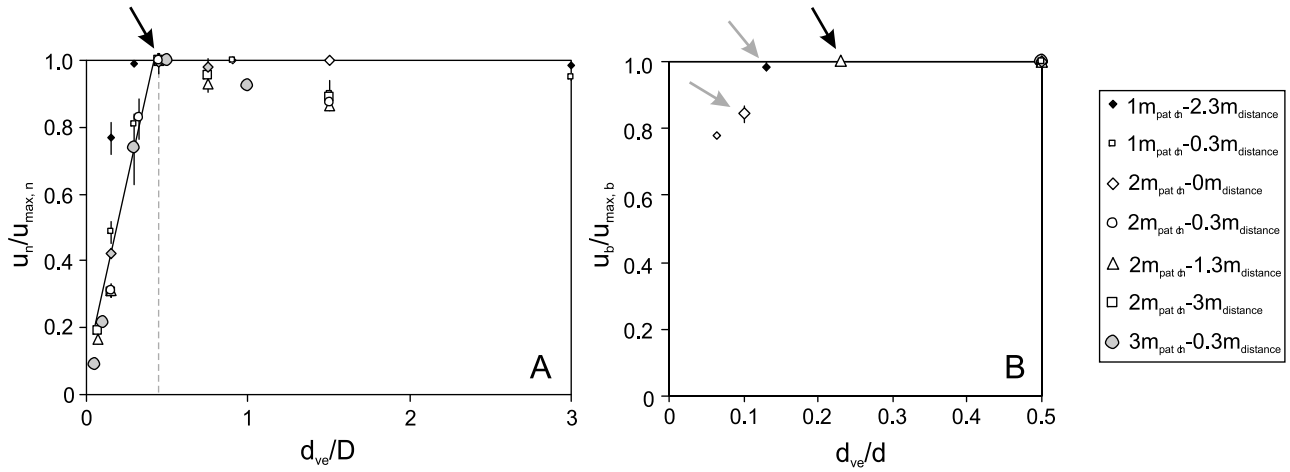

Figure 7. Spatial variation in flow velocity presented in a dimensionless way. (a) Effect of patch size on the spatial variation in flow velocity next to the patches. (b) Effect of interpatch distance on the spatial variation in flow velocity in between the patches.

edge there is a decrease in flow velocity; farther away there is an increase (Figure 4). Second, the flow patterns are clearly affected by patch size (Figures 4a and 4b), while little effect is observed for the interpatch distance (Figure 4c). To quantify the effect of patch size on the spatial variation in flow velocity next to the patch, a dimensionless analysis was performed, including all data points next to the patches (Figure 7a). For values of the dimensionless distance from the patch $d_{ve}/D \leq 0.45$ (left of the dashed line in Figure 7a), the measured flow velocity increases with d_{ve}/D, until the maximum flow velocity is reached at $d_{ve}/D = 0.45$ (four of the seven configurations plot at this point, see the black arrow in Figure 7a). The following relationship is then observed for $d_{ve}/D \leq 0.45$ (Figure 7a, solid line):

$$\frac{u_n}{u_{\max,n}} = b\left(\frac{d_{ve}}{D}\right)^c + d, \tag{2}$$

where u_n is the measured flow velocity at distance d_{ve}/D next to the patch (m/s), $u_{\max,n}$ is the maximum measured flow velocity next to the patch (m/s); d_{ve} is the distance from the vegetation edge (m), and b, c, and d are regression coefficients. In this case, next to a square *Spartina anglica* patch, $b = 2.201$, $c = 1$, and $d = 0.074$ ($R^2 = 0.86$; $p < 0.0001$). Equation (1), which describes the effect of patch size on the maximum flow velocity, can be rewritten as

$$u_{\max,n} = \exp\left(a\frac{D}{h}\right)u_{inc} \tag{3}$$

by substituting $u_{\max,n}$ in equation (2) with equation (3), the following relationship is found:

$$u_n = \exp\left(a\frac{D}{h}\right)\left[b\left(\frac{d_{ve}}{D}\right)^c + d\right]u_{inc}. \tag{4}$$

In this way the flow velocity next to the patch (u_n), at a given distance from the vegetation edge (d_{ve}), can be predicted solely based on the incoming flow velocity (u_{inc}) and the patch diameter (D), taking into account that equation (4) is only valid if $d_{ve}/D \leq 0.45$.

[24] For $d_{ve}/D > 0.45$, data points plot in a different way (right of the dashed line in Figure 7a). There maximum flow velocities may occur up to $d_{ve}/D = 1.5$ (only for one configuration), and in general $u_n/u_{\max,n} \geq 0.85$ for all data points. At a certain distance from the vegetation edge there will no longer be patch-flow interaction; there $u_n = u_{inc}$. We did not observe this threshold distance in our experiments (at $d_{ve} = 0.3$ m, $u_n > u_{inc}$ for all patch configurations; see Figure 4).

[25] Similar to the dimensionless analysis of the flow patterns *next to* the patches described above, we performed a dimensionless analysis including all data points *in between* the patches, in order to quantify the effect of interpatch distance (d) on the spatial flow pattern in between patches (Figure 7b). Here the maximum flow velocity is reached at $d_{ve}/d = 0.23$ (Figure 7b, black arrow). A significant decrease in measured flow velocities is observed for a d_{ve}/d value between 0.13 and 0.1 (Figure 7b, gray arrows). If we consider, e.g., 2 m patches at an interdistance of 1 m, the maximum flow velocity in between the patches occurs at 0.23 m from the vegetation edge ($d_{ve}/d = 0.23$) and the flow velocity significantly decreases only close to the vegetation edge at 0.10 m ($d_{ve}/d = 0.1$). Next to the patches the maximum flow velocity is reached at $d_{ve}/D = 0.45$ (Figure 7a, black arrow) and thus for a 2 m patch at a distance of 0.9 m from the vegetation edge. For $d_{ve}/D < 0.45$ the flow velocity next to the patch immediately decreases according to equation (2) (see solid black line in Figure 7a) and reaches much lower $u/u_{\max}$ values than in between the patches. This example illustrates that in between interacting patches, the flow becomes concentrated. As opposed to the model next to the patches, we could not construct a significant model in between the patches.

3.6. Flow Interaction in Between Patches

[26] Except for the 1 m patches at 2.3 m interdistance, all patch configurations have an asymmetrical flow pattern, by which we mean that the spatial flow pattern in between the patches differs from the spatial flow pattern next to the patches (Figure 4). We consider that there is flow interaction in between two adjacent patches, when the flow patterns

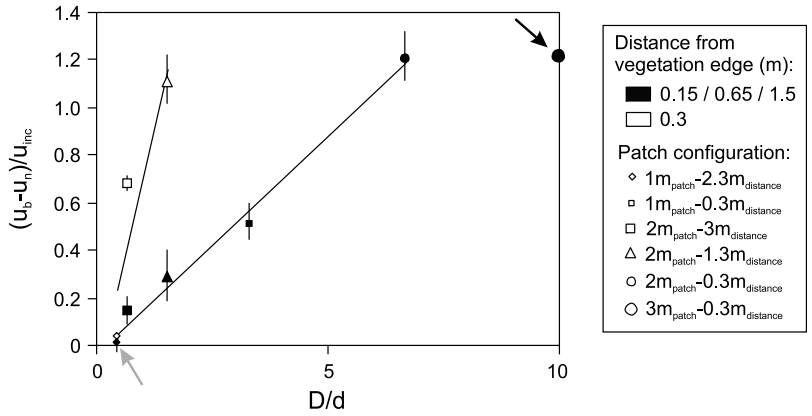

Figure 8. Degree of flow interaction $(u_b - u_n)/u_{inc}$ as a function of the lateral patch growth D/d.

next to and in between the patches are asymmetrical. The degree of flow interaction is quantified here as the difference in flow velocities next to and in between the patches, measured at a same distance from the vegetation edge. This dimensionless measure for the degree of flow interaction, $(u_b - u_n)/u_{inc}$, was related then to a dimensionless measure for lateral patch growth, D/d (Figure 8). For the 1 m patches at 2.3 m interdistance (D/d = 0.43; Figure 8, gray arrow), $(u_b - u_n)/u_{inc}$ values are close to zero (at both 0.15 and 0.3 m), indicating that flow interaction in between patches is absent. Indeed, for this configuration, the observed flow patterns next to and between the patches are symmetrical (Figure 4a, 1 m_{patch}-2.3 $m_{distance}$). However, with increasing lateral patch growth (i.e., increasing values of D/d), the degree of flow interaction increases (i.e., $(u_b - u_n)/u_{inc}$ values increase), whereby the strongest increase occurs at 0.3 m from the vegetation edge (cf. both trend lines in Figure 8). Considering the measurements at 0.15, 0.65, and 1.5 m, one patch configuration does not follow the observed trend (i.e., 3 m_{patch}-0.3 $m_{distance}$; see Figure 8, black arrow). There the flow interaction is lower as expected, caused by the suppressing of the flow velocity (see Figure 6, in between). We infer that from a given D/d value between 6.67 and 10 patch growth suppresses the increase in flow velocity in between patches.

3.7. Comparing Square and Circular Patch Shapes

[27] The flow patterns next to a square patch and a circular patch were very comparable (Figure 9). There is no significant difference in flow velocity for all measuring locations, except at 0.3 m from the vegetation edge where the flow velocity for a circular patch is higher. This may imply that the increase in flow velocity next to circular patches occurs closer to the vegetation edge and that flow interaction in between circular patches occurs at smaller interpatch distances. Nevertheless, the flow patterns for both shapes were very similar and we may conclude that our experiments with square patches are also representative for circular patches, as observed more commonly in the field.

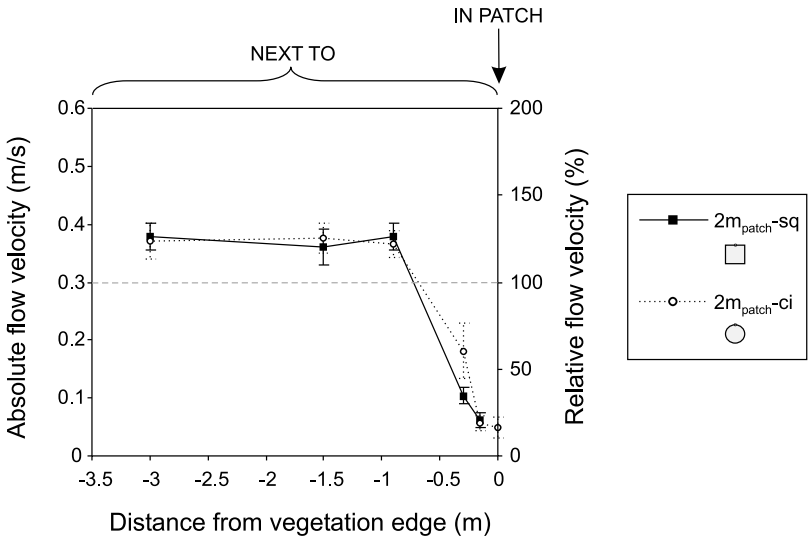

Figure 9. Effect of patch shape: comparison of flow velocities (m/s and %) next to a square patch and a circular patch.

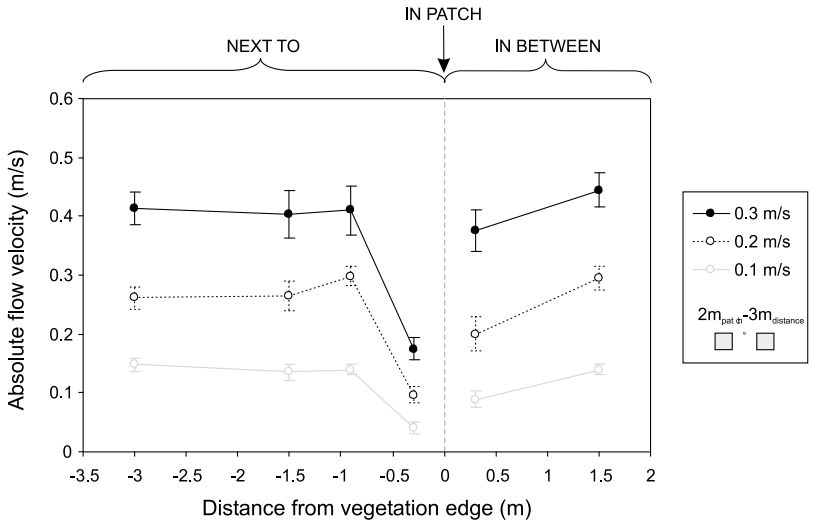

Figure 10. Effect of incoming flow velocity. Absolute flow velocities (m/s) plotted against the distance from the vegetation edge (m) for the three incoming flow velocities.

3.8. Effect of Varying Incoming Flow Velocity

[28] By using a single patch configuration, the effect of different incoming flow velocities was tested. The relative increase and decrease of flow velocities around the patches was not significantly different for all three incoming flow velocities. However, the initiation of erosion and the limitation of plant growth are determined by the absolute flow velocities. It is clear that the absolute increase in flow velocity increases with greater incoming flow velocity (Figure 10).

4. Discussion

[29] The importance of biogeomorphic feedback between vegetation, flow, and landform changes is increasingly recognized for many landscape types [*Corenblit et al.*, 2008; *Murray et al.*, 2008]. While most biogeomorphic studies so far have been based on models in which vegetation is considered to reduce flow velocities and reduce erosion [e.g., *D'Alpaos et al.*, 2007; *Istanbulluoglu and Bras*, 2005], we showed empirically that flow reduction is only a local effect within and close to vegetation patches, while flow acceleration dominates next to and between the patches. In the field, it has been demonstrated that this flow acceleration next to *Spartina anglica* patches may initiate at some point the erosion of channels [*Bouma et al.*, 2007; *Van Hulzen et al.*, 2007] and thereby limit the further lateral growth of the vegetation [*van Wesenbeeck et al.*, 2008]. As the patch size D in our experiments became larger and the interdistance d smaller, the patches started to interact ($D/d \geq 0.43$–0.67), and ultimately, when patch size and interdistance passed a second critical threshold ($D/d \geq 6.67$–10), the flow acceleration in between the patches again decreased (Figure 6). This implies that, once this second critical threshold is passed, the merging of two growing adjacent patches is no longer hindered by flow acceleration. For the outside, next to the patches, we found a positive relationship between the amount of flow acceleration and the patch size (Figure 6), suggesting that channel formation is more likely around larger patches. This is supported by field data, showing that deeper channels occur next to larger *S. anglica* patches [*van Wesenbeeck et al.*, 2008]. The formation of deeper channels next to laterally growing patches may limit at some point the further expansion of the patch. In the field, experiments with *S. anglica* transplants showed that the survival and growth of the transplants was strongly suppressed in the channels [*van Wesenbeeck et al.*, 2008].

[30] Our results on flow interaction between nearby vegetation patches qualitatively agree with general theory on flow around cylindrical, nonpermeable flow-blocking structures (e.g., bridge piles or abutments). For such structures, flow interaction was reported at $D/d > 0.25$–0.5 (D is pile diameter; d is pile interdistance), depending on the pile-group arrangement [*Ataie-Ashtiani and Beheshti*, 2006]. For *Spartina anglica* vegetation patches, we found that flow interaction occurs when $D/d \geq 0.43$–0.67 (Figure 8). For piles with a side-by-side arrangement (as in our experiments), the piles were found to act as a single pile at $D/d > 4$ [*Ataie-Ashtiani and Beheshti*, 2006], while we observed decreased flow interaction between *S. anglica* patches for $D/d \geq 6.67$–10 (Figure 8). The critical threshold values that we report are higher for vegetation patches than for piles, likely because piles are nonpermeable structures while vegetation patches may be regarded as a porous structure. This effect of porosity is important for vegetation patches with different vegetation densities (e.g., caused by different plant species morphology or different stem densities): with increasing vegetation density, we expect that more water is forced to flow around the vegetation patches, resulting in flow interaction between adjacent patches starting for lower D/d values. As a consequence, vegetation patches with higher vegetation densities will have stronger effects on biogeomorphic landscape evolution (e.g., stronger flow concentration and channel erosion in between growing vegetation patches) [*Temmerman et al.*, 2007].

[31] In between interacting *Spartina anglica* patches we always observed flow acceleration and flow concentration (Figure 7b). However, what determines now if growing patches can merge together or not? The answer for this probably lies in the larger scale landscape process. Our

experiments demonstrate that, for a range of incoming flow velocities, the relative flow acceleration will always remain the same. However, the absolute flow velocity next to and in between the patches depends on the absolute value of the incoming flow (Figure 10). Therefore, for patches that occur at more sheltered sites, where the incoming flow velocities are lower (e.g., by a high density of surrounding patches), the accelerated flow around the patches remains in absolute terms too low to initiate scouring, which has been shown to be velocity dependent [*van Wesenbeeck et al.*, 2008]. At these sites, *Spartina* patches can easily merge together and eventually form closed *Spartina* fields. However, if patches are more exposed, incoming flow velocities are higher and absolute flow acceleration will be sufficiently large to initiate channel formation and to limit further lateral patch growth. The newly formed channels may develop further and evolve toward the larger tidal channels that typically dissect intertidal marsh vegetation [*Temmerman et al.*, 2007]. This explanation is supported by time series of aerial photographs, indicating that at some locations the lateral growth of *Spartina* patches is limited by increasing flow-induced erosion next to the patches, while at other locations this limitation does not occur and patches grow together (Figure 1b).

[32] In our flume study we always used two square patches that were placed next to each other relative to the incoming flow direction. In the field, more complex situations may occur: the patches are mostly circular in shape (but this had no significant effect on our results, see Figure 9), more complex configurations of more than two patches may occur, and the direction of the incoming flow velocity may be variable.

[33] Our study focused on the intertidal landscape; however, our results may also have implications for other landscape types. Some similar effects on flow concentration and channel formation have been reported for other landscapes that are affected by flowing water and by the colonization of patchy vegetation. For example, *Coulthard* [2005] mentioned the formation of erosion gullies next to vegetation patches in a scaled flume study on alluvial channel braiding. In a more extended flume experiment, it has been demonstrated that plant colonization on the floodplain of a braiding river may concentrate the flow to a single river channel [*Gran and Paola*, 2001; *Tal and Paola*, 2007]. In addition, flow deviation around vegetation patches was also reported for other landscape types, such as hillslopes [e.g., *Bochet et al.*, 2000], high dynamic rivers with emergent vegetation [e.g., *Schnauder and Moggridge*, 2009], and more low dynamic rivers with submerged vegetation [e.g., *Cotton et al.*, 2006]. In the latter, an extensive study of the bed morphology showed channel formation in between vegetation patches.

5. Conclusions

[34] Our study quantified the amount and spatial patterns of flow acceleration next to and between dynamically growing vegetation patches of *Spartina anglica* (Figures 6–8 and equations (1)–(4)). We quantified that the flow acceleration next to vegetation patches and the distance from the vegetation patch where maximum flow acceleration occurs increase with increasing patch size (respectively Figure 6 and equation (1), Figure 7 and equation (2)). We found that flow interaction in between two patches started as soon as $D/d \geq 0.43$–0.67 (D is patch size; d is interpatch distance). Further patch growth (increasing D/d) resulted in increasing flow acceleration in between the patches, until a second critical condition was reached, at $D/d \geq 6.67$–10, where flow acceleration was suppressed and the two patches started to act as one. These findings are in accordance with general theory on flow around and between nonpermeable structures, such as bridge piles and abutments; however, the threshold D/d values reported here for flow interaction and flow suppression are higher than those for nonpermeable structures, due to the permeability of the vegetation patches. The reported interactions between flow hydrodynamics and dynamic vegetation patches will be essential to further understanding of the larger-scale biogeomorphic evolution of tidal landscapes, and other landscapes affected by flowing water and colonized by patchy vegetation, such as river floodplains, river beds, and hillslopes. Our study provides clear empirical evidence that such scale-dependent biogeomorphic feedback should be included in models describing the formation and evolution of landscapes.

Notation

d interpatch distance, m.
d_{ve} distance from the vegetation edge, m/s.
D patch diameter, m.
h water depth, m.
u flow velocity, m/s.
u_b flow velocity in between the patches, m/s.
u_{inc} incoming flow velocity, m/s.
$u_{\max}$ maximum flow velocity, m/s.
$u_{\max,b}$ maximum flow velocity in between the patches, m/s.
$u_{\max,n}$ maximum flow velocity next to the patch, m/s.
u_n flow velocity next to the patch, m/s.

[35] **Acknowledgments.** This work has been supported by the EU 6th Framework Programme, Integrated Infrastructure Initiative HYDRALAB III within the Transnational Access Activities, contract 022441. We are grateful to all European partners involved in this HYDRALAB project, especially Suzanna Ilic (Lancaster University), Ivan Caceres and Tiago Oliveira (Polytechnical University of Catalunya), and Massimo Guerero and Alberto Lamberti (University of Bologna), for thoughtful discussions and practical assistance. We thank Bas Koutstaal for plant maintenance and Daphne van der Wal for providing georeferenced aerial photographs. We also wish to thank several anonymous referees whose comments improved this paper substantially.

References

Ataie-Ashtiani, B., and A. A. Beheshti (2006), Experimental investigation of clear-water local scour at pile groups, *J. Hydraul. Eng.*, *132*(10), 1100–1104, doi:10.1061/(ASCE)0733-9429(2006)132:10(1100).

Baas, A. C. W., and J. M. Nield (2007), Modelling vegetated dune landscapes, *Geophys. Res. Lett.*, *34*(6), L06405, doi:10.1029/2006GL029152.

Bochet, E., J. Poesen, and J. L. Rubio (2000), Mound development as an interaction of individual plants with soil, water erosion and sedimentation processes on slopes, *Earth Surf. Processes Landforms*, *25*, 847–867, doi:10.1002/1096-9837(200008)25:8<847::AID-ESP103>3.0.CO;2-Q.

Bouma, T. J., M. B. De Vries, E. Low, L. Kusters, P. M. J. Herman, I. C. Tanczos, S. Temmerman, A. Hesselink, P. Meire, and S. van Regenmortel (2005), Flow hydrodynamics on a mudflat and in salt marsh vegetation: Identifying general relationships for habitat characterisations, *Hydrobiologia*, *540*, 259–274, doi:10.1007/s10750-004-7149-0.

Bouma, T. J., L. A. Van Duren, S. Temmerman, T. Claverie, A. Blanco-Garcia, T. Ysebaert, and P. M. J. Herman (2007), Spatial flow and sedimentation patterns within patches of epibenthic structures: Combining

field, flume and modelling experiments, *Cont. Shelf Res.*, *27*, 1020–1045, doi:10.1016/j.csr.2005.12.019.

Bouma, T. J., M. Friedrichs, B. K. van Wesenbeeck, S. Temmerman, G. Graf, and P. M. J. Herman (2009), Density-dependent linkage of scale-dependent feedbacks: A flume study on the intertidal macrophyte *Spartina anglica*, *Oikos*, *118*(2), 260–268, doi:10.1111/j.1600-0706.2008.16892.x.

Callaway, J. C., and M. N. Josselyn (1992), The introduction and spread of smooth cordgrass (*Spartina alterniflora*) in South San Francisco Bay, *Estuaries*, *15*, 218–226, doi:10.2307/1352695.

Collins, D. B. G., R. L. Bras, and G. E. Tucker (2004), Modeling the effects of vegetation-erosion coupling on landscape evolution, *J. Geophys. Res.*, *109*, F03004, doi:10.1029/2003JF000028.

Corenblit, D., A. M. Gurnell, J. Steiger, and E. Tabacchi (2008), Reciprocal adjustments between landforms and living organisms: Extended geomorphic evolutionary insights, *Catena*, *73*(3), 261–273, doi:10.1016/j.catena.2007.11.002.

Cotton, J. A., G. Wharton, J. A. B. Bass, C. M. Heppell, and R. S. Wotton (2006), The effects of seasonal changes to in-stream vegetation cover on patterns of flow and accumulation of sediment, *Geomorphology*, *77*, 320–334, doi:10.1016/j.geomorph.2006.01.010.

Coulthard, T. J. (2005), Effects of vegetation on braided stream pattern and dynamics, *Water Resour. Res.*, *41*, W04003, doi:10.1029/2004WR003201.

D'Alpaos, A., S. Lanzoni, M. Marani, and A. Rinaldo (2007), Landscape evolution in tidal embayments: Modeling the interplay of erosion, sedimentation, and vegetation dynamics, *J. Geophys. Res.*, *112*, F01008, doi:10.1029/2006JF000537.

Gran, K., and C. Paola (2001), Riparian vegetation controls on braided stream dynamics, *Water Resour. Res.*, *37*, 3275–3283, doi:10.1029/2000WR000203.

Hubbard, J. C. E. (1965), *Spartina* marshes in southern England. VI. Pattern of invasion in Poole Harbour, *J. Ecol.*, *53*, 799–813, doi:10.2307/2257637.

Istanbulluoglu, E., and R. L. Bras (2005), Vegetation-modulated landscape evolution: Effects of vegetation on landscape processes, drainage density, and topography, *J. Geophys. Res.*, *110*, F02012, doi:10.1029/2004JF000249.

Kirwan, M. L., and A. B. Murray (2007), A coupled geomorphic and ecological model of tidal marsh evolution, *Proc. Natl. Acad. Sci. U. S. A.*, *104*(15), 6118–6122, doi:10.1073/pnas.0700958104.

Leonard, L. A., and A. L. Croft (2006), The effect of standing biomass on flow velocity and turbulence in *Spartina alterniflora* canopies, *Estuarine Coastal Shelf Sci.*, *69*, 325–336, doi:10.1016/j.ecss.2006.05.004.

Leonard, L. A., and M. E. Luther (1995), Flow hydrodynamics in tidal marsh canopies, *Limnol. Oceanogr.*, *40*(8), 1474–1484, doi:10.4319/lo.1995.40.8.1474.

Marani, M., A. D'Alpaos, S. Lanzoni, L. Carniello, and A. Rinaldo (2007), Biologically controlled multiple equilibria of tidal landforms and the fate of the Venice lagoon, *Geophys. Res. Lett.*, *34*, L11402, doi:10.1029/2007GL030178.

Melville, B. W. (1997), Pier and abutment scour: Integrated approach, *J. Hydraul. Eng.*, *123*(2), 125–136, doi:10.1061/(ASCE)0733-9429(1997)123:2(125).

Melville, B. W., and Y. M. Chiew (1999), Time scale for local scour at bridge piers, *J. Hydraul. Eng.*, *125*(1), 59–65, doi:10.1061/(ASCE)0733-9429(1999)125:1(59).

Murray, A. B., and C. Paola (2003), Modelling the effect of vegetation on channel pattern in bedload rivers, *Earth Surf. Processes Landforms*, *28*, 131–143, doi:10.1002/esp.428.

Murray, A. B., M. A. F. Knaapen, M. Tal, and M. L. Kirwan (2008), Biomorphodynamics: Physical-biological feedbacks that shape landscapes, *Water Resour. Res.*, *44*, W11301, doi:10.1029/2007WR006410.

Nepf, H. M., and E. R. Vivoni (2000), Flow structure in depth-limited, vegetated flow, *J. Geophys. Res.*, *105*(C12), 28,547–28,557, doi:10.1029/2000JC900145.

Neumeier, U., and C. L. Amos (2006), The influence of vegetation on turbulence and flow velocities in European salt-marshes, *Sedimentology*, *53*(2), 259–277, doi:10.1111/j.1365-3091.2006.00772.x.

Oliveto, G., and W. H. Hager (2002), Temporal evolution of clear-water pier and abutment scour, *J. Hydraul. Eng.*, *128*(9), 811–820, doi:10.1061/(ASCE)0733-9429(2002)128:9(811).

Rietkerk, M., and J. Van de Koppel (2008), Regular pattern formation in real ecosystems, *Trends Ecol. Evol.*, *23*(3), 169–175, doi:10.1016/j.tree.2007.10.013.

Sanchez, J. M., D. G. SanLeon, and J. Izco (2001), Primary colonisation of mudflat estuaries by *Spartina maritima* (Curtis) Fernald in northwest Spain: Vegetation structure and sediment accretion, *Aquat. Bot.*, *69*(1), 15–25, doi:10.1016/S0304-3770(00)00139-X.

Schnauder, I., and H. Moggridge (2009), Vegetation and hydraulic-morphological interactions at the individual plant, patch and channel scale, *Aquat. Sci.*, *71*(3), 318–330, doi:10.1007/s00027-009-9202-6.

Shi, Z., J. S. Pethick, and K. Pye (1995), Flow structure in and above the various heights of a saltmarsh canopy: A laboratory flume study, *J. Coastal Res.*, *11*, 1204–1209.

Shi, Z., J. S. Pethick, F. Burd, and B. Murphy (1996), Velocity profiles in a salt marsh canopy, *Geo-Mar. Lett.*, *16*, 319–323, doi:10.1007/BF01245563.

Tal, M., and C. Paola (2007), Dynamic single-thread channels maintained by the interaction of flow and vegetation, *Geology*, *35*, 347–350, doi:10.1130/G23260A.1.

Temmerman, S., T. J. Bouma, G. Govers, Z. B. Wang, M. B. De Vries, and P. M. J. Herman (2005), Impact of vegetation on flow routing and sedimentation patterns: Three-dimensional modeling for a tidal marsh, *J. Geophys. Res.*, *110*, F04019, doi:10.1029/2005JF000301.

Temmerman, S., T. J. Bouma, J. Van de Koppel, D. Van der Wal, M. B. De Vries, and P. M. J. Herman (2007), Vegetation causes channel erosion in a tidal landscape, *Geology*, *35*(7), 631–634, doi:10.1130/G23502A.1.

Van Hulzen, J. B., J. Van Soelen, and T. J. Bouma (2007), Morphological variation and habitat modification are strongly correlated for the autogenic ecosystem engineer *Spartina anglica* (common cordgrass), *Estuaries Coasts*, *30*(1), 1–19.

van Wesenbeeck, B. K., J. van de Koppel, P. M. J. Herman, and T. J. Bouma (2008), Does scale-dependent feedback explain spatial complexity in salt-marsh ecosystems?, *Oikos*, *117*(1), 152–159, doi:10.1111/j.2007.0030-1299.16245.x.

T. Balke, T. J. Bouma, and P. C. Klaassen, Centre for Estuarine and Marine Ecology, Netherlands Institute of Ecology, NL-4400 AC Yerseke, Netherlands. (Thorsten.Balke@deltares.nl; t.bouma@nioo.knaw.nl; p.klaassen@nioo.knaw.nl)

G. Biermans, P. Meire, J. Schoelynck, S. Temmerman, and W. Vandenbruwaene, Department of Biology, University of Antwerp, B-2610 Wilrijk Antwerpen, Belgium. (gbierman@sckcen.be; patrick.meire@ua.ac.be; jonas.schoelynck@ua.ac.be; stijn.temmerman@ua.ac.be; wouter.vandenbruwaene@ua.ac.be)

D. P. Callaghan, School of Civil Engineering, University of Queensland, Brisbane, 4072 Qld, Australia. (dave.callaghan@uq.edu.au)

F. Dekker, M. B. de Vries, E. Martini, L. A. van Duren, and P. van Steeg, Deltares, Postbus 177, NL-2600 MH Delft, Netherlands. (Mindert.deVries@deltares.nl; Erika.Martini@deltares.nl; luca.vanduren@deltares.nl; paul.vansteeg@deltares.nl)